3. Wave system を用いた遺伝子診断

高橋政代[1)]、万代道子[1)]、平見恭彦[2)]、横田友子[1)]、鈴木拓也[2)]
村上智昭[2)]、大音壮太郎[2)]、秋元正行[1)]、小杉真司[3)]、吉村長久[2)]
([1)]京都大探索医療センター 、[2)]京都大、 [3)]京都大社会健康医学系医療倫理学)

研究要旨 網膜色素変性は原因遺伝子が多岐にわたり、あらゆる遺伝形式をとる疾患である。遺伝歴から判断することが難しい場合や孤発例も多く、遺伝形式不明例が多い。そこで、多くの原因遺伝子を簡便に解析するために、WAVE システムを用いてスクリーニングした後、シークエンスを行う方法を検討した。この方法により網膜色素変性患者１００例中９例に原因遺伝子の可能性が高いヘテロの変異が確認され、そのうち５例は遺伝形式不明であったことから遺伝形式特定に寄与できる可能性があると思われた。

A．研究目的

網膜色素変性には様々な遺伝形式が存在するが、孤発例や遺伝形式不明例も多い。遺伝子診断により遺伝形式を特定することができるが、原因遺伝子は多岐にわたるため候補遺伝子すべての変異を検索するのは困難である。我々は遺伝子検索の効率を高めるために Transgenic 社製の WAVE system を用いる遺伝子診断システムを採用し、網膜色素変性患者の遺伝子変異を検出できたので報告する。

B．研究方法

対象は当院通院中の網膜色素変性患者のうち遺伝形式に関わらず同意を得られた100名。患者末梢血を採取、DNA を抽出し、WAVE system を用いて現在網膜色素変性の原因遺伝子として報告されている29遺伝子 110 エクソンの遺伝子変異についてスクリーニングした。WAVE によって遺伝子変異の有無を検索し、変異を認めたエクソンに対してシークエンスを行った。

（倫理面への配慮）

本研究は京都大学「医の倫理委員会」の承認を受けている。患者に対しては DNA の利用目的と方法について十分説明を行い、同意を得て採血した。

C．研究結果

100 例中優性遺伝子のみのスクリーニングは 10 例、劣性遺伝子のみのスクリーニングは 14 例、大部分の 76 例は遺伝歴からは形式が確定できず優性、劣性両方の遺伝子をスクリーニングした。

100 例全体で WAVE 解析は 9628 解析、そのうち波形変化あるいは結果不明瞭でシークエンスしたものは 2030 解析（21%）、シークエンスによって SNP または延期変異の確認できたものは 269 解析（13%）であった。現在までに 9 例で疾患の原因と考えられる遺伝子変異が同定された。変異遺伝子は RDS 4例、rhodopsin 3例、FSCN2 2 例で、いずれもヘテロの変異であった。９例中５例は家族歴からは遺伝形

式が特定できなかった症例であった。

D．考察

ID	gene	exon	mutation
37	FSCN2	1	208 DelG
56	RDS	1	Met152Val
59	RHO	3	Gly188Arg
61	RHO	2	Gly174Ser
63	RHO	2	Arg135Trp
66	RDS	1	Ala 116 Ser
75	FSCN2	1	208 DelG
85	RDS	1	Met152Val
93	RDS	1	Gly167Ser

WAVE system を用いた遺伝子診断は１人の患者の候補遺伝子を一挙に検索でき、簡便さとコストの点で優れた方法と思われた。

E．結論

今後親族の遺伝子診断を進める必要があるが、遺伝形式不明の場合も遺伝子診断により遺伝形式を特定できる可能性がある。

F．健康危険情報

なし

G．研究発表

１．論文発表

なし

２．学会発表

ARVO meeting 2004.5 (Florida)
M.Mandai, S.Kosugi, Y.Hirami, T.Yokota, N.Kawagoe, M.Takahashi.: Trial to Introduce an Economic and Efficcient System for Genetic Diagnosis in Patients in Kyoto University Hospital.

H．知的財産権の出願・登録状況

１．特許取得

なし

２．実用新案登録

なし

３．その他

なし

I．参考文献

1. Nickerson, M.L., Weirich, G., Zbar, B., and Schmidt, L.S. Signature-based analysis of MET proto-oncogene mutations using DHPLC.Hum. Mutat. 16: 68-76, 2000.
2. Prasad S, Kolln KA, Cucci RA, Trembath RC, Van Camp G, Smith RJ. Pendred syndrome and DFNB4-mutation screening of SLC26A4 by denaturing high-performance liquid chromatography and the identification of eleven novel mutations.Am. J. Med. Genet. 124A: 1-9, 2004.

4. *PRPF31*遺伝子変異による常染色体優性網膜色素変性家系における見かけ上の不完全浸透

中澤　満、平　紅、佐藤元哉
(弘前大)

研究要旨　常染色体優性網膜色素変性（ADRP）家系の中には明らかに遺伝子異常を持っていることが確実であるにもかかわらず夜盲などの臨床症状を欠く症例の存在が知られている。そのような症例の存在が知られる家系の一つに19番染色体長腕19q13.4に連鎖するものがありこれをRP11という。今回の研究では我々が既報でRP11であることを報告した日本人1家系における候補遺伝子PRPF31遺伝子の変異（1142delG）を同定し、さらに本家系の中で夜盲などの臨床症状を持たない2症例にも同一の遺伝子変異があることを確認した。また、この2症例では種々の程度に網膜変性や視細胞障害がみられることから、自覚症状を持たなくとも軽度の網膜変性を示しており、これらの症例は「見かけ上の不完全浸透」であることが明らかとなった。

A．研究目的

常染色体優性網膜色素変性（ADRP）の原因遺伝子 *PRPF31*（19q31.4)はスプライシング機構に関係するタンパク質をコードし、その変異をもつADRP家系（RP11）には遺伝子変異をもちながら臨床症状（夜盲などの自覚症状）のない症例が存在する[1]。このような現象を不完全浸透と称する場合もあるようであるが、不完全浸透の場合は自覚症状を欠く症例は臨床上全く正常な表現型を示すことが条件となる。我々は以前からRP11家系でみられる遺伝子変異を持ちながら臨床症状のない症例がどのような分子機構によって起こるのかを明らかにすることを目的として検索を進めているが、今回は我々がかつて報告したRP11家系での候補遺伝子 *PRPF31* 遺伝子における変異の存在の確認と異常遺伝子型を有する症例の臨床所見の詳細を検討したので報告する。とくに留意したのはPRPF31遺伝子変異の実際と自覚症状を欠く症例が臨床上全く正常表現型なのか、または軽度の網膜色素変性所見を呈するのかどうかという点である。

B．研究方法

連鎖解析にて19番染色体19q31.4に連鎖することが明らかな既報[1,2]のADRP1家系7名について候補遺伝子 *PRPF31* の全コード領域をポリメラーゼ連鎖法（PCR法）にて増幅し、PCR法にプライマーとして用いたオリゴヌクレオチドを用いて直接塩基配列決定法を行い塩基配列を決定し、変異検索を行った。塩基配列はABI社プリズム301を使用した。

臨床所見については矯正視力、細隙灯顕微鏡による前眼部・中間透光体所見、検眼鏡

による眼底所見、蛍光眼底撮影、動的視野および網膜電図（ERG）所見にて検討した。

C．結果

臨床上典型的な網膜色素変性を示す５名と夜盲の自覚のない２名全例に *PRPF31* 遺伝子に 1142 番目のグアニン塩基の一塩基欠失変異(1142delG)をヘテロ接合で認めた。一塩基欠失であるので、この変異によってフレームシフトを生じ、この変異より下流に 30 個の異常アミノ酸残基を生じた後終止コドンとなる。なお正常対照５０名には同変異はみられなかった。

臨床所見では夜盲の自覚のある症例では全例、10 歳台の比較的早期に夜盲を自覚しはじめ、年齢とともに視野狭窄の進行があり、眼底には典型的な網膜色素変性像を呈していた。夜盲の自覚のない２名では１例には眼底所見および蛍光眼底所見は正常であるものの視野にて内部イソプターの沈下とERG a 波の振幅の軽度低下がみられ、他の１例には周辺部の網膜色素上皮萎縮と視野狭窄および ERG a 波の明らかな振幅低下がみられ、種々の程度に網膜機能が障害されていた。これらの所見を総合すると *PRPF31* 遺伝子変異があるにもかかわらず夜盲などの自覚症状のない症例でも種々の程度に軽度の網膜変性ないしは視細胞機能の障害がみられることが明らかとなった。

D．考察

これまで *PRPF31* 遺伝子変異 ADRP（RP11）の臨床像として、自覚症状のない症例では臨床像は全く正常であるという報告もあったが、[3, 4] 1142delG 変異では種々の程度に変性がみられることが明らかとなり、これらの所見を総合すると、典型的な「不完全浸透」ではなく少なくとも「見かけ上の不完全浸透」と称されるべき現象であることが分かった。同一遺伝子の同一変異を持ちながら症例によって臨床像にこのような多様性を示す原因としては、正常アレルの *PRPF31* 遺伝子発現の量的変化の差のためである可能性が示唆されており、[5] 遺伝子変異の存在のみならず今後は種々のレベルでの遺伝子発現の量的変化を含めた検索が必要であることが示された。

E．結論

PRPF31 遺伝子 1142delG 変異を持ちながら夜盲などの自覚症状のない症例でも臨床的に軽度の網膜変性や視細胞機能異常がみられ、これらの症例は見かけ上の不完全浸透ともいうべき変化であることが明らかになった。今後、PRPF31 遺伝子発現の量的検索による発症機構の解明の必要性が示唆された。

F．健康危険情報

なし

G．研究発表

１．　論文発表

1. Takaya K, Suzuki Y, Mizutani H,

Sakuraba T, Nakazawa M.
Long-term results of vitrectomy for removal of submacular hard exudates in patients with diabetic maculopathy. Retina, 24, 23-29, 2004.

2. Usui T, Ichibe M, Tanimoto N, Ueki S, Takagi M, Hasegawa S, Abe H, Miyagawa Y, Nakazawa M.The ocular fundus observed by scanning laser ophthalmoscopy in a patient with enhanced S-cone syndrome. Retina, 24, 946-952, 2004..
3. Takano Y, Ohguro H, Dezawa M, Ishikawa H, Yamazaki H, Ohguro I, Mamiya K, Metoki T, Ishikawa F, Nakazawa M. Study of drug effects of calcium channel blockers on retinal degeneration of rd mouse. Biochem Biophys Res Com, 313, 1015-1022, 2004.
4. Usui T, Tanimoto N, Ueki S, Takagi M, Hasegawa S, Abe H, Sekiya K, Nakazawa M. Rod a-wave in Oguchi disease. Vision Research, 44, 535-540, 2004.
5. Ohguro H, Odagiri H, Miyagawa Y, Ohguro I, Sasaki M, Nakazawa M. Clinicopathological features of gastric cancer cases and aberrantly expressed recoverin. Tohoku J exp Med, 202, 213-219, 2004.
6. Ohguro H, Yokoi Y, Ohguro I, Mamiya K, Ishikawa F, Yamazaki H, Metoki T, Takano Y, Ito T, Nakazawa M. Clinical and Immunologic aspects of cancer-associated retinopathy. Am J Ophthalmol, 137 (6), 1117-1119, 2004.
7. Sato M, Nakazawa M, Usui T, Tanimoto N, Abe H, Ohguro H. Mutations in the gene coding for guanylate cyclase-activating protein 2 (*GUCA1B* gene) in patients with autosomal dominant retinal dystrophies. Graefes Arch Clin Exp Ophthalmol in press.
8. Mamiya K, Ohguro H, Ohguro I, Metoki T, Miyagawa Y, Ishikawa F, Yamazaki H, Takano Y, Ito T, Nakazawa M. Effects of MMC III gene transfer by electroporation in glaucoma filter surgery. Exp Eye Res, 79 (7), 405-410, 2004.

2. 学会発表

1. 山崎仁志、大黒　浩、石川　太、目時友美、高野淑子、伊藤　忠、中沢　満. RCS ラットの網膜変性に対する Ca 拮抗剤の効果. 第 108 回日本眼科学会総会、東京、2004.
2. 高野淑子、大黒　浩、大黒幾代、間宮和久、山崎仁志、石川　太、目時友美、伊藤　忠、中沢　満. Rd マウス網膜に

対するカルシウム拮抗剤の影響.　第108回日本眼科学会総会、東京、2004.

3. 間宮和久、大黒　浩、目時友美、大黒幾代、石川　太、中沢　満.　緑内障治療における結膜MMPsとTIMPsの動態とその効果.　第108回日本眼科学会総会、東京、2004.

4. 高谷　香、鈴木幸彦、中沢　満.　ウサギを用いた経硝子体網膜静脈カニュレーションの組織学的検討.　第108回日本眼科学会総会、東京、2004.

5. 鈴木幸彦、高谷　香、目時友美、中澤　満.　術後の水晶体嚢収縮により支持部が光学部から分離した眼内レンズの光学顕微鏡所見.　第108回日本眼科学会総会、東京、2004.

6. 石川　太、大黒　浩、大黒幾代、間宮和久、目時友美、山崎仁志、高野淑子、伊藤　忠、中澤　満.　遺伝性網膜変性疾患モデルラットへのlight-stressの影響.　第108回日本眼科学会総会、東京、2004.

7. 平　紅、中沢　満、佐藤元哉.　PRPF31遺伝子変異による常染色体優性網膜色素変性家系の見かけ上の不完全浸透.　第58回日本臨床眼科学会総会、東京、2004.

8. 中澤　満.　遺伝性網膜変性疾患の臨床と基礎研究（特別講演）.　第42回北日本眼科学会、福島、2004.

H．知的財産権の出願・登録状況

1．特許取得

なし

2．実用新案登録

なし

3．その他

なし

I．参考文献

なし

5. 変異解析を行った卵黄様黄斑ジストロフィの1例

塩瀬聡美、吉田茂生、山地陽子、石橋達朗
(九州大)

研究要旨　卵黄様黄斑ジストロフィ(以下VMD)は常染色体優性の疾患で、眼底所見は病期によって変化し、診断には、眼球電図(EOG)が有用である。近年その原因遺伝子としてVMD2が報告されている。欧米では80例を越える報告があるが、本邦ではその変異解析の報告はyanagiらの2例のみである[1]。眼底、EOGの所見からVMDと考えられた患者のVMD2遺伝子解析を行ったところ、Ala195Val変異を認めた。これはインターネットのVMD2 Mutation Database (http://www.uniwuerzburg.de/humangenetics/vmd2.html) で海外で既に報告されている[2]変異と同一であった。近年公のデータベースが充実し、変異解析が容易になっているので、VMDの診断確定と病態の把握に遺伝子解析が有用であると考えられた。

A. 研究目的

VMD患者にVMD2遺伝子解析を行うこと。

症例：37歳女性。平成16年1月より左眼で小さい字が見にくいとの主訴で当科初診。家族内に明らかなVMD患者はなく、既往歴に特記事項なし。初診時、視力右眼1.2、左眼0.8(矯正不能)で眼圧、前眼部、中間透光体は正常。両眼底に黄色の隆起性病変とその周囲の網膜色素上皮 (RPE) 萎縮からなる2/3乳頭径大の病巣を認めた。周辺網膜に異常はなかった。蛍光眼底造影ではFAで黄色沈着部はblockによる低蛍光を、RPE萎縮部はwindow defectによる過蛍光を示した。IAでも黄色沈着部に一致したblockによる低蛍光を示した。視野、色覚、および錐体、桿体ERGは異常なく、multifocal ERGでは両眼黄斑機能が低下していた。光干渉断層計(OCT3)では黄色沈着物とおもわれる、視細胞層とRPE層の間の紡錘形の高反射体を認めた。EOGは平坦型で、L/D比は右眼1.5左眼1.3と軽度低下していた。以上の、いり卵様眼底所見、EOGの平坦化、ERG正常から、VMDと診断した。同意を得て、患者末梢血を用いたdirect sequence解析をVMD2遺伝子の解析を行ったところ、VMD2 Mutation Databaseで既報告のAla195Val変異を認めた。

D. 考察

近年の分子遺伝学的研究の進歩で公のデータベースが充実し、変異解析が容易になってきた。本症例では眼底、EOGの所見からVMDの診断が可能であったが、一般にVMDは浸透率があまり高くなく、また、病初期は正常眼底のことがあり、特に小児は病初期のことが多く、EOGの施行が難しい場合がある。このような場合は遺伝子診断が診断確定に有用と考えられた。

VMD2のコードする蛋白はbestrophinと呼ばれる68kDaの蛋白で、網膜色素上皮のbasolateral membraneに存在すると考え

られており[3]、EOG の light peak に関与するクロライドチャンネルであるといわれている[4]。本症例では bestrophin の 4 ヶ所の膜貫通部位のうち 2 番と 3 番の間の細胞内 domain に存在するアミノ酸の変異が存在した。それにより、bestrophin 蛋白の構造が変化し、そのクロライドチャンネルとしての機能に異常が生じ、網膜色素上皮細胞内のイオンの不均衡がおこり EOG が平坦化したと考えられた。
また、イオンの不均衡は RPE の老廃物の排泄機能を障害し、神経網膜下に OCT で見られたような沈着物が生じたと考えられた。

E．結論　日本人 VMD 患者で VMD2 Mutation Database で既に報告されている変異を認めた。公のデータベースを用いて変異同定を容易に行えた。VMD2 のコードするクロライドチャンネルの機能異常が EOG 平坦化や、沈着物の原因と考えられた。VMD の診断確定と病態の把握に遺伝子解析が有用であると考えられた。

F．健康危険情報

なし

G．研究発表

1．論文発表

なし

2．学会発表

なし

H．知的財産権の出願・登録状況

1．特許取得

なし

2．実用新案登録

なし

3．その他

なし

I．参考文献

1. Yanagi Y, Sekine H, Mori M. Identification of a novel VMD2 mutation in Japanese patients with Best disease. Ophthalmic Genet. 23: 129-133, 2002.
2. AJ Lotery, FL Munier, GA Fishman et al. Allelic variation in the VMD2 gene in Best disease and age-related macular degeneration. IOVS 41: 1291-1296, 2000.
3. Marmorstein AD, Marmorstein LY, Rayborn M et al. Bestrophin, the product of the Best vitelliform macular dystrophy gene (VMD2), localizes to the basolateral plasma membrane of the retinal pigment epithelium. Proc. Nat. Acad. Sci 97: 12758-12763, 2000.
4. Sun H, Tunenari T, Yau KW, Nathans J. The vitelliform macular dystrophy protein defines a new family of chloride channels. Proc. Nat. Acad. Sci. 99:4008-4013, 2002.

6. GeneChip を用いた転写因子 Nrl の標的遺伝子の同定

吉田茂生[1)]、吉田綾子[1)]、山地陽子[1)]、Anand Swaroop[2)]
Carrolee Barlow[3)]、石橋達朗[1)]
([1)]九州大、[2)] ミシガン大、[3)] ソーク研究所)

研究要旨 桿体特異的 Neural retina leucine zipper (Nrl)蛋白は桿体の分化に重要で、Nrl 欠損マウス(以下 $Nrl^{-/-}$)ではすべての桿体の錐体への形質転換がおこる。今回、Nrl によって発現が制御される標的遺伝子群を把握するため、網膜発達段階での $Nrl^{-/-}$の遺伝子発現プロファイリングを行った。生後 2 日、10 日、2 ヶ月の $Nrl^{-/-}$およびワイルドタイプコントロールマウス(以下 WT)の網膜より RNA を抽出し、ビオチンで標識した cRNA ターゲットを合成し、Affymetrix GeneChip (MGU74Av2)にハイブリダイズした。スキャン画像を定量後、各グループ間で発現レベルの異なる遺伝子群を抽出した。さらに時系列の階層的クラスタリングにより抽出分子群を分類した。$Nrl^{-/-}$と WT 網膜間で 161 の遺伝子が有意な発現レベルの差を認めた。抽出遺伝子群は、光トランスダクション、シグナル伝達、転写制御、細胞内物質輸送などの機能単位に分類できた。このうち 41 遺伝子はヒト染色体上の網膜疾患の連鎖領域に存在した。抽出遺伝子群は、錐体と桿体の差異あるいは桿体の欠失による網膜の再構成を反映しており、その一部はヒト網膜疾患の候補遺伝子となりうると考えた。本研究により、視細胞の分化に伴う制御機構の一部が明らかになった。

A. 研究目的

種々の網膜神経細胞は網膜神経前駆細胞に由来し、その分化は内因性の遺伝的プログラムや、細胞をとりまく特異的な微小環境によって誘導される。視細胞の分化や機能維持に関わる遺伝子発現ネットーワークを網羅的、体系的に解明することは、新たなヒト網膜疾患の原因遺伝子の同定や、将来の網膜再生医療にむけた重要な知見につながることが期待される。

近年の研究により、網膜細胞の分化に関与する転写因子が次第に明らかになっている。NRL (Neural Retina Leucine zipper)は大 Maf-family に属する bZIP 型の転写因子で、転写因子 CRX と共役してロドプシンのプロモーターに結合し、桿体への分化誘導に関与する。また、Nrl のホモ欠損マウス (以下 $Nrl^{-/-}$)ではすべての桿体の錐体への形質転換がおこる。今回、Nrl によって発現が制御される標的遺伝子群を把握するため、網膜発達段階での $Nrl^{-/-}$の遺伝子発現プロファイリングを行った。

B. 研究方法

生後 2 日、10 日、2 ヶ月の $Nrl^{-/-}$およびワイルドタイプコントロールマウス(以下 WT)の網膜より RNA を抽出し、ビオチンで標識した cRNA ターゲットを合成し、Affymetrix

GeneChip (MGU74Av2)にハイブリダイズした。ハイブリダイズは各グループごとに異なるサンプルを用いて 4 回繰り返し、スキャン画像を定量後、各グループ間で発現レベルの異なる遺伝子群を抽出した。さらに時系列の階層的クラスタリングにより抽出分子群を分類した。

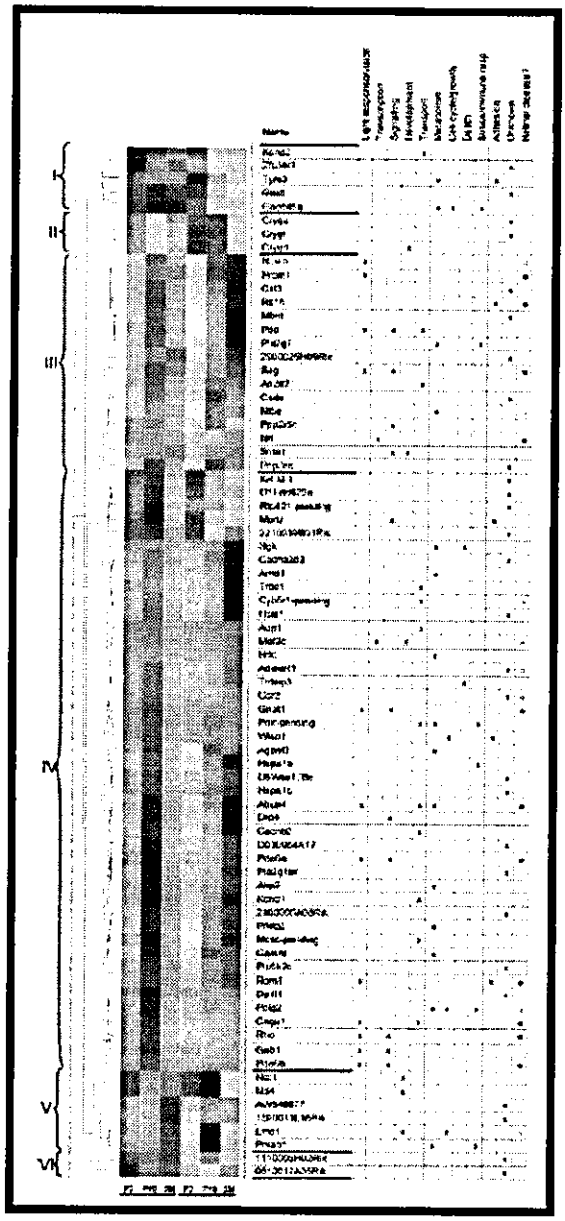

図 1　階層的クラスタリングと機能アノテーション

（倫理面への配慮）

動物の取り扱いにあたっては、ARVO の動物取り扱いガイドラインを遵守した。

C．研究結果

$Nrl^{-/-}$と WT 網膜間で 161 の遺伝子が有意な発現レベルの差を認めた。この結果は定量的 real-time PCR の結果とよく相関していた。抽出遺伝子群は、光トランスダクション、シグナル伝達、転写制御、細胞内物質輸送などの機能単位に分類できた(図 1)。このうち 41 遺伝子はヒト染色体上の網膜疾患の連鎖領域に存在した。抽出遺伝子群のクロマチン免疫沈降法では、光トランスダクション関連遺伝子のみならず、より広範囲の機能的遺伝子が in　vivo で Nrl により直接的に制御されていた(図 2) 。

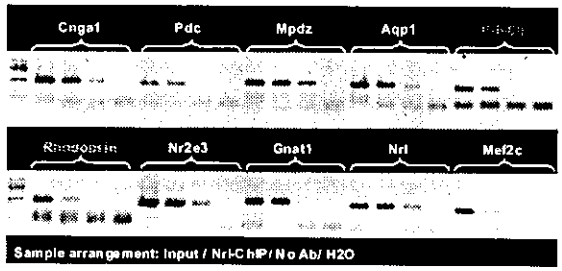

図 2　クロマチン免疫沈降法

D．考察

今回の解析で、視細胞の発生（生後 2 日)、分化(10 日)あるいは機能維持 (2 ヶ月）に関与する遺伝子が部分的に同定されたと考えている。抽出された光トランスダクション、転写制御因子、シグナル伝達や発生に関与する遺伝子群は、錐体と桿体の差異あるいは桿体の欠失による網膜の再構成を反映していると考えられる。また、その一部はヒト網膜疾患の候補遺伝子となる可能性があ

る。

今回、マイクロアレイとクロマチン免疫沈降法を組み合わせることで、様々な Nrl の直接的な標的遺伝子を同定した。この中には、種々の錐体と桿体の分化に関与すると考えられる転写因子が含まれていた。本研究同様に、Crx、Trβ2、Nr2e3 など他の視細胞分化に深く関わる転写因子の機能欠失マウスを用いた網膜遺伝子プロファイリングを行い、これらを整理、統合することで、網膜の分化や機能維持の制御ネットワークに関するきわめて重要な知見が得られると考えている。

E．結論

本研究により、視細胞の分化に伴う制御機構の一部が明らかになった。

F．健康危険情報

なし

G．研究発表

1．論文発表

1. Yoshida S, et al. Expression profiling of the developing and mature Nrl-/- mouse retina: identification of retinal disease candidates and transcriptional regulatory targets of Nrl. Hum Mol Genet 13,1487-1503,2004.

2．学会発表

1. Mears AJ, et al. Identification of the downstream targets of Nrl: the key regulator of rod photoreceptor differentiation. Association for Research in Vision and Ophthalmology, Fort Lauderdale,2004.

H．知的財産権の出願・登録状況

1．特許取得

なし

2．実用新案登録

なし

3．その他

なし

I．参考文献

1. Swaroop A, et al. A conserved retina-specific gene encodes a basic motif/leucine zipper domain. Proc Natl Acad Sci U S A 89,266-270,1992.

2. Mears AJ, et al. Nrl is required for rod photoreceptor development. Nat Genet 29,447-452,2001.

3.Yu J, et al. Altered expression of genes of the Bmp/Smad and Wnt/calcium signaling pathways in the cone-only Nrl-/- mouse retina, revealed by gene profiling using custom cDNA microarrays. J Biol Chem 279,42211-42220,2004.

Human Molecular Genetics, 2004, Vol. 13, No. 14 **1487–1503**
DOI: 10.1093/hmg/ddh160
Advance Access published on May 26, 2004

Expression profiling of the developing and mature Nrl$^{-/-}$ mouse retina: identification of retinal disease candidates and transcriptional regulatory targets of Nrl

Shigeo Yoshida[1,†,‡], Alan J. Mears[1,†,¶], James S. Friedman[1], Todd Carter[4], Shirley He[1], Edwin Oh[1], Yuezhou Jing[2], Rafal Farjo[1,§], Gilles Fleury[5], Carrolee Barlow[4,‖], Alfred O. Hero[2] and Anand Swaroop[1,3,*]

[1]Department of Ophthalmology and Visual Sciences, [2]Departments of EECS, Biomedical Engineering and Statistics and [3]Department of Human Genetics, University of Michigan, Ann Arbor, MI, USA, [4]The Salk Institute for Biological Studies, San Diego, California, USA and [5]Service des Mesures Ecole Supérieure d'Electricité, Gif-sur-Yvette, France

Received March 20, 2004; Revised and Accepted May 14, 2004

The rod photoreceptor-specific neural retina leucine zipper protein Nrl is essential for rod differentiation and plays a critical role in regulating gene expression. In the mouse retina, rods account for 97% of the photoreceptors; however, in the absence of Nrl (Nrl$^{-/-}$), no rods are present and a concomitant increase in cones is observed. A functional all-cone mouse retina represents a unique opportunity to investigate, at the molecular level, differences between the two photoreceptor subtypes. Using mouse GeneChips (Affymetrix), we have generated expression profiles of the wild-type and Nrl$^{-/-}$ retina at three time-points representing distinct stages of photoreceptor differentiation. Comparative data analysis revealed 161 differentially expressed genes; of which, 78 exhibited significantly lower and 83 higher expression in the Nrl$^{-/-}$ retina. Hierarchical clustering was utilized to predict the function of these genes in a temporal context. The differentially expressed genes primarily encode proteins associated with signal transduction, transcriptional regulation, intracellular transport and other processes, which likely correspond to differences between rods and cones and/or retinal remodeling in the absence of rods. A significant number of these genes may serve as candidates for diseases involving rod or cone dysfunction. Chromatin immunoprecipitation assay showed that in addition to the rod phototransduction genes, Nrl might modulate the promoters of many functionally diverse genes *in vivo*. Our studies provide molecular insights into differences between rod and cone function, yield interesting candidates for retinal diseases and assist in identifying transcriptional regulatory targets of Nrl.

INTRODUCTION

The mammalian retina contains a diverse array of anatomically and functionally distinct neurons (1). Rod and cone photoreceptors account for >70% of all cells in the retina. In most mammals, rods are almost 20-fold more in number compared with cones though their distribution may vary greatly in different regions (2). Photoreceptors are highly metabolically active post-mitotic neurons; it is estimated that almost 10 billion opsin molecules are synthesized per

*To whom correspondence should be addressed at: Department of Ophthalmology and Visual Sciences and Department of Human Genetics, W.K. Kellogg Eye Center, University of Michigan, 1000 Wall Street, Ann Arbor, MI 48105-0714, USA. Tel: +1 7347633731; Fax: +1 7346470228; Email: swaroop@umich.edu
†The authors wish it to be known that, in their opinion, the first two authors should be regarded as joint First Authors.
‡Present address: Department of Ophthalmology, Kyushu University Graduate School of Medical Sciences, Fukuoka, Japan.
¶Present address: University of Ottawa Eye Institute and Ottawa Health Research Institute, Ottawa, Ontario, Canada.
§Present address: Department of Cell Biology, University of Oklahoma Health Sciences Center, Oklahoma City, OK, USA.
‖Present address: Merck Research Laboratories, San Diego, CA, USA.

second in each human retina (3). Hence, it is not surprising that altered expression or function of opsin and other phototransduction proteins results in photoreceptor degeneration (4–6). The transcriptional regulatory networks underlying photoreceptor differentiation and function are understood poorly.

The neural retina leucine zipper (Nrl) protein, a transcription factor of the Maf-subfamily, is expressed specifically in the rod photoreceptors of the retina (7,8) and the pineal gland (A.J. Mears and A. Swaroop, unpublished data). Nrl has been shown to interact with the retina-specific homeodomain protein Crx (9) and regulate the expression of rhodopsin (10) and rod cGMP-phosphodiesterase α- (11) and β-subunits (12). In humans, missense mutations of *NRL* are associated with autosomal dominant retinitis pigmentosa (13–17), and in at least one instance (Ser50Thr mutation), the disease may be a result of increased activity of the NRL protein. Targeted deletion of Nrl in mice results in a complete loss of rods and a supernormal S-cone function, as demonstrated by histology, immunocytochemistry, ERG and expression analysis (18). These observations led to the hypothesis that Nrl plays a critical role in the differentiation of rod photoreceptors, and in its absence, the immature photoreceptors adopt an S-cone phenotype (18). The retina of the $Nrl^{-/-}$ mouse exhibits similarities to the *Nr2e3*^{rd7} mouse (19,20) and its corresponding human disease enhanced S-cone syndrome (21). One plausible explanation of the phenotypic overlap is that Nrl directly or indirectly regulates Nr2e3 expression, which is undetectable in the $Nrl^{-/-}$ mouse retina (18).

Although several transcription factors have been implicated in photoreceptor differentiation or gene regulation (22–25), their direct impact on the photoreceptor transcriptome has not been elucidated. Microarray-based global expression profiling of tissues from mice deficient in a transcription factor gene can point to downstream regulatory targets and provide candidate genes for functional studies and cloning of disease loci (26). This approach has been utilized successfully in studies of the mouse retina (27,28). The $Nrl^{-/-}$ retina is particularly amenable to this analysis because of its dramatic phenotype of no rods and enhanced cones. In the retina of $Nrl^{-/-}$ mice, rod bipolar cells have normal morphology, pattern of staining and lamination, and form functional connections with the cones, and the axonal arbors of horizontal cells and AII amacrine cells maintain a normal morphology and stratification pattern (E. Strettoi, A.J. Mears and A. Swaroop, unpublished data). We, therefore, hypothesize that the comparative analysis of gene profiles from the wild-type and $Nrl^{-/-}$ retina will, to a large extent, reveal expression differences between rod and cone transcriptomes. Based on our initial analysis of phototransduction genes (18), we predict that transcripts encoding rod photoreceptor proteins would be expressed at lower levels (or undetectable) in the $Nrl^{-/-}$ retina. Conversely, the transcripts specific to the normally sparse population of cones are expected to be enriched in the $Nrl^{-/-}$ retina.

Here, we report the gene expression profiles, obtained by using Affymetrix GeneChips (MGU74Av2), of the wild-type and $Nrl^{-/-}$ retina at three time-points (post-natal days 2 and 10, and 2 months). After data normalization by robust multichip average algorithm (RMA) (29) and ranking the statistically validated genes with a minimum 1.5 average fold-change (AFC) in expression, we have identified 161 differentially expressed genes, which include the known rod- or cone-specific genes represented on these chips. Functional annotation suggests a wide spectrum of physiological changes that likely correspond to differences between rods and cones and/or remodeling of retina in the absence of rods. Our analysis suggests that ~25% of all differentially expressed genes identified in this study are either associated with (15) or are candidates (26) for retinal diseases. Using chromatin immunoprecipitation (ChIP) analysis, a significant proportion of the top ranked genes showing reduced expression in the $Nrl^{-/-}$ retina are demonstrated to be putative direct targets of Nrl, indicating the breadth of its influence on the rod transcriptome.

RESULTS

Identification of differentially expressed genes in the $Nrl^{-/-}$ retina

The three time-points, P2, P10 and 2 months, were chosen to cover distinct critical stages of photoreceptor development in mouse. In the wild-type retina, at P2 many retinal progenitor cells are still exiting the cell cycle and a majority of these will become rods (30). The photopigment of the rod photoreceptors, rhodopsin, is first detected at P4. At P10, retinogenesis is complete, the cells are undergoing terminal differentiation and photoreceptor outer segments are beginning to form. We chose 2 months of age as another suitable time-point as the retina is structurally and functionally matured and yet old enough to avoid any potential delayed differentiation effects which may occur due to the re-specification of the photoreceptor cell types in the $Nrl^{-/-}$ retina.

To facilitate statistical analysis and identification of 'true' positives, four replicate MGU74Av2 GeneChips were utilized for each time-point and strain. Based on absent/present calls (MAS5 analysis), ~60% of the probesets (out of ~12 400) were reported as present or marginally detectable in at least one of the 12 wild-type GeneChips, consistent with other studies analyzing single tissue types. Signal quantification and normalization were performed using RMA, a reliable and effective algorithm in control studies (31,32). The normalized data were then analyzed with a robust two-step procedure to identify statistically significant differentially expressed genes. Due to the tendency of microarrays to quantitatively underestimate fold-change in expression and since RMA normalization compresses the signals (and resulting ratios), an empirical 1.5 AFC cut-off was selected as the minimum fold-change (minfc) for statistical analysis. Using these criteria and after removal of those scored as absent on all 24 chips, a total of 173 probesets were reported as differentially expressed for at least one of the three time-points (i.e. *P*-value < 1). Of these, 86 show decreased (Table 1, down-regulated genes) and 87 increased (Table 1, up-regulated genes) expression in the $Nrl^{-/-}$ retina. The differentially expressed genes are ranked based on increasing false discovery rate confidence interval (FDRCI) *P*-values, which are similar to FDR *P*-values except that they account for a specified minfc level in

Table 1. Summary of microarray-based expression

Probeset	Accession no.	Gene description	Name	P2 AFC	P10 AFC	2M AFC	*P*-value
Down-regulated genes							
96134_at	NM_139292	Deleted in polyposis 1-like 1	Dp1l1	—	−10.12	−15.94	0.0001
96567_at	NM_145383	Rhodopsin	Rho	—	−24.82	−41.30	0.0001
94701_at	NM_008806	Phosphodiesterase 6B, cGMP, rod receptor, beta polypeptide	Pde6b	*−2.29*	−37.30	−25.00	0.0002
95389_at	XM_132106	Cyclic nucleotide gated channel alpha 1	Cnga1	—	−7.25	−13.63	0.0004
93453_at	NM_009073	Retinal outer segment membrane protein 1	Rom1	−2.17	−5.32	−3.27	0.0004
94853_at	NM_008142	Guanine nucleotide binding protein, beta 1	Gnb1	*1.17*	−4.01	−8.12	0.0004
98531_g_at	NM_013525	Growth arrest specific 5	Gas5	*−1.15*	*−2.08*	−6.28	0.0008
94139_at	NM_024458	Phosducin	Pdc	−4.41	−3.84	−1.91	0.0008
93330_at	NM_007472	Aquaporin 1	Aqp1	—	*−1.33*	−7.84	0.0011
104592_i_at	NM_025282	Myocyte enhancer factor 2C	Mef2c	—	—	−4.18	0.0029
161871_f_at	NM_145383	Rhodopsin	Rho**	—	−2.95	−7.80	0.0030
94150_at	NM_009118	Retinal S-antigen	Sag	−5.07	−4.10	*−1.20*	0.0037
99860_at	NM_008140	Guanine nucleotide binding protein, alpha transducing 1	Gnat1	*−1.19*	−55.61	−216.35	0.0046
95755_at	NM_011733	Cold shock domain protein A	Csda	*1.13*	*−1.51*	−2.25	0.0059
161525_f_at	NM_009073	Retinal outer segment membrane protein 1	Rom1**	*1.04*	−4.76	−3.70	0.0060
162167_f_at	NM_008806	Phosphodiesterase 6B, cGMP, rod receptor, beta polypeptide	Pde6b**	—	−3.74	−4.99	0.0060
93533_at	NM_026899	RIKEN cDNA *1500011L16* gene	1500011L16Rik	*−1.06*	−2.62	*−1.72*	0.0065
93699_at	NM_015810	Polymerase (DNA directed), gamma 2, accessory subunit	Polg2	*−1.01*	−1.73	−3.64	0.0069
93094_at	NM_007672	Cerebellar degeneration-related 2	Cdr2	*−1.07*	−2.99	−5.47	0.0080
104591_g_at	NM_025282	Myocyte enhancer factor 2C	Mef2c**	—	—	−2.53	0.0080
101923_at	NM_013737	Phospholipase A2, group VII	Pla2g7	*−1.03*	−2.57	*−1.82*	0.0115
96831_at	NM_028295	Protein disulfide isomerase-related	Pdir-pending	*−1.02*	*−1.14*	−2.68	0.0120
103895_at	NM_145930	Expressed sequence AW549877	AW549877	*1.03*	−2.08	*−1.30*	0.0130
92796_at	NM_007431	Alkaline phosphatase 2, liver	Akp2	—	−3.10	−3.17	0.0144
100696_at	NM_008805	Phosphodiesterase 6A, cGMP-specific, rod, alpha	Pde6a	—	*−2.12*	−2.95	0.0160
102890_at	NM_009228	Syntrophin, acidic 1	Snta1	*−1.07*	−2.74	−2.37	0.0194
160273_at	NM_007565	Zinc finger protein 36, C3H type-like 2	Zfp36l2	*1.41*	−1.96	−3.68	0.0197
160134_at	XM_129394	Adiponectin receptor 1	AdipoR1	*−1.20*	*−1.42*	−2.73	0.0248
98853_at	NM_008867	Phospholipase A2, group IB, pancreas, receptor	Pla2g1br	—	−3.13	−2.82	0.0254
100946_at	XM_286803	Heat shock protein 1B	Hspa1b	—	*−1.19*	−3.17	0.0269
104590_at	NM_025282	Myocyte enhancer factor 2C	Mef2c**	—	—	−3.66	0.0295
93875_at	XM_207062	Heat shock protein 1A	Hspa1a	*−1.05*	*−1.19*	−2.62	0.0296
92691_at	NM_028392	RIKEN cDNA *2900026H06* gene	2900026H06Rik	*−1.41*	−3.19	*−1.23*	0.0340
97730_at	NM_007378	ATP-binding cassette, sub-family A (ABC1), member 4	Abca4	*−1.43*	−2.76	−2.22	0.0347
103733_at	AK013486	RIKEN cDNA *2900006A08* gene	2900006A08Rik	*1.00*	*−1.49*	−1.96	0.0383
102044_at	NM_018865	WNT1 inducible signaling pathway protein 1	Wisp1	—	*−1.23*	−3.33	0.0479
102612_at	NM_008736	Neural retina leucine zipper gene	Nrl	—	−2.59	−2.48	0.0510
99392_at	NM_009397	Tumor necrosis factor, alpha-induced protein 3	Tnfaip3	—	−2.12	−4.52	0.0580
95541_at	NM_138587	DNA segment, Chr 6, Wayne State University 176, expressed	D6Wsu176e	*1.00*	*−1.43*	−3.27	0.0650
160807_at	NM_053014	1-Acylglycerol-3-phosphate *O*-acyltransferase 3	Agpat3	*−1.08*	*−1.10*	−2.27	0.0700
98300_at	NM_009785	Calcium channel, voltage dependent, alpha2/delta subunit 3	Cacna2d3	—	*1.00*	−2.08	0.0780
93390_g_at	NM_008935	Prominin 1	Prom1	*1.00*	−1.86	*−1.64*	0.0810
160597_at	NM_133825	DNA segment, Chr 1, ERATO Doi 622, expressed	D1Ertd622e	*1.09*	*−1.33*	−2.46	0.0934
160693_at	NM_054097	Phosphatidylinositol-4-phosphate 5-kinase, type II, gamma	Pip5k2c	*−1.08*	−1.90	−2.21	0.0980
97890_at	NM_011361	Serum/glucocorticoid regulated kinase	Sgk	*−1.09*	*−1.02*	−2.69	0.0980
93328_at	NM_008230	Histidine decarboxylase	Hdc	—	—	−2.12	0.1070
93887_at	NM_010820	Multiple PDZ domain protein	Mpdz	*1.06*	*−1.50*	−2.60	0.1084
104206_at	NM_026153	RIKEN cDNA *0610012A05* gene	0610012A05Rik	*−2.07*	−5.70	−2.66	0.1195
96596_at	NM_008681	N-myc downstream regulated-like	Ndrl	*−1.05*	−1.78	−2.64	0.1370
102292_at	NM_007836	Growth arrest and DNA-damage-inducible 45 alpha	Gadd45a	*1.10*	−2.15	−2.32	0.1450
160948_at	NM_008915	Protein phosphatase 3, catalytic subunit, gamma isoform	Ppp3cc	*1.01*	*−1.07*	−2.27	0.1578

Continued

Table 1. *Continued*

Probeset	Accession no.	Gene description	Name	P2 AFC	P10 AFC	2M AFC	*P*-value
97770_s_at	NM_138587	DNA segment, Chr 6, Wayne State University 176, expressed	D6Wsu176e**	*1.20*	*−1.27*	−2.84	0.1610
160464_s_at	NM_010884	N-myc downstream regulated 1	Ndr1	*−1.08*	−1.82	−2.60	0.1819
94739_at	NM_011643	Transient receptor potential cation channel, subfamily C, member 1	Trpc1	*1.00*	*−1.13*	−2.55	0.1948
97755_at	NM_007878	Dopamine receptor 4	Drd4	—	−4.54	−2.46	0.2070
101151_at	NM_009038	Recoverin	Rcvrn	—	−2.37	−2.12	0.2120
97357_at	AK044589	Myocyte enhancer factor 2C	Mef2c**	—	—	−2.39	0.2140
96354_at	NM_020007	Muscleblind-like (*Drosophila*)	Mbnl1	*1.05*	−2.02	*−1.47*	0.2530
95603_at	NM_138595	Glycine decarboxylase	Gldc	*−1.13*	−2.15	*1.17*	0.2840
102413_at	NM_057173	LIM domain only 1	Lmo1	*−1.16*	*−1.54*	−1.87	0.2940
98993_at	NM_012023	Protein phosphatase 2, regulatory subunit B (B56), gamma isoform	Ppp2r5c	*−1.08*	*−1.45*	−2.12	0.3280
93130_at	NM_183212	Hypothetical protein D030064A17	D030064A17	*1.04*	*−1.68*	−1.96	0.3570
93389_at	NM_008935	Prominin 1	Prom1**	*1.01*	−1.82	*−1.64*	0.3640
93202_at	NM_011851	5′ Nucleotidase, ecto	Nt5e	*1.09*	*−2.07*	−2.65	0.3720
95285_at	XM_128499	KRAB box containing zinc finger protein	KRIM-1	*1.05*	*−1.12*	−1.84	0.4030
102352_at	NM_134189	*N*-Acetylgalactosaminyltransferase 9	Galnt9	*1.03*	*−1.28*	−1.80	0.4760
98569_at	NM_146118	Mitochondrial Ca^{2+}-dependent solute carrier	Mcsc-pending	*−1.18*	*−1.47*	−1.98	0.4830
99461_at	NM_008225	Hematopoietic cell specific Lyn substrate 1	Hcls1	—	—	−1.90	0.4850
97579_f_at	NM_027010	Crystallin, gamma F	Crygf	*1.82*	*2.46*	−3.51	0.4940
160808_at	NM_031869	Protein kinase, AMP-activated, beta 1 non-catalytic subunit	Prkab1	*−1.15*	*−1.55*	−2.13	0.5120
101308_at	NM_008420	Potassium voltage gated channel, Shab-related subfamily, member 1	Kcnb1	—	−2.14	−2.43	0.5120
103026_f_at	NM_007777	Crystallin, gamma E	Cryge	*1.74*	*2.24*	−3.07	0.5220
98524_f_at	AK008780	RIKEN cDNA *2210039B01* gene	2210039B01Rik	*1.02*	*−1.58*	−2.26	0.5290
98329_at	XM_193953	6-Phosphofructo-2-kinase/ fructose-2,6-biphosphatase 2	Pfkfb2	—	*−1.47*	−1.77	0.5697
103460_at	NM_029083	HIF-1 responsive RTP801	Rtp801-pending	*1.00*	*−1.17*	−2.14	0.5980
100757_at	XM_194003	Calcium channel, voltage-dependent, beta 2 subunit	Cacnb2	—	−2.23	*−1.81*	0.6290
102835_at	NM_007459	Adaptor protein complex AP-2, alpha 2 subunit	Ap2a2	*1.02*	*−1.52*	−1.83	0.6490
99586_at	NM_009976	Cystatin C	Cst3	*−1.07*	−1.71	*−1.60*	0.6940
96156_at	AK003573	RIKEN cDNA *1110008H02* gene	1110008H02Rik	*−3.21*	−2.38	−4.42	0.7627
104171_f_at	NM_007776	Crystallin, gamma D	Crygd	*1.83*	*2.37*	−3.16	0.7652
96766_s_at	NM_019392	TYRO3 protein tyrosine kinase 3	Tyro3	*−1.16*	*−1.07*	−1.63	0.7750
101489_at	NM_009665	*S*-Adenosylmethionine decarboxylase 1	Amd1	*1.20*	*−1.04*	−1.80	0.8460
103922_f_at	NM_028057	Cytochrome b5 reductase 1 (B5R.1)	Cyb5r1-pending	*1.11*	*−1.42*	−2.04	0.8540
92790_at	NM_010655	Karyopherin (importin) alpha 2	Kpna2	*1.30*	*−1.35*	−1.97	0.8670
92607_at	NM_008590	Mesoderm specific transcript	Mest	*1.41*	*1.08*	−2.02	0.9058
101702_at	NM_011302	Retinoschisis 1 homolog (human)	Rs1h	—	−2.70	*−1.59*	0.9617
Up-regulated genes							
92237_at	NM_009107	Retinoid X receptor gamma	Rxrg	*−1.01*	2.50	2.92	0.0000
160893_at	NM_023121	Guanine nucleotide binding protein, gamma transducing activity pp 2	Gngt2	*1.14*	6.20	7.90	0.0001
98807_at	NM_008141	Guanine nucleotide binding protein, alpha transducing 2	Gnat2	*1.48*	7.20	7.58	0.0002
162287_r_at	NM_017474	Chloride channel calcium activated 3	Clca3	—	3.20	14.88	0.0003
99395_at	NM_007538	Opsin 1 (cone pigments), short-wave-sensitive	Opn1sw	*1.29*	8.43	9.40	0.0004
102151_at	NM_007419	Adrenergic receptor, beta 1	Adrb1	*1.16*	4.33	4.55	0.0007
98498_at	NM_007611	Caspase 7	Casp7	*1.06*	1.75	6.36	0.0017
98499_s_at	NM_007611	Caspase 7	Casp7**	*−1.05*	*1.67*	5.93	0.0023
96920_at	NM_019564	Protease, serine, 11 (Igf binding)	Prss11	*1.13*	2.30	*1.36*	0.0023
98427_s_at	NM_008689	Nuclear factor of kappa light chain gene enhancer in B-cells 1, p105	Nfkb1	*1.05*	1.81	3.05	0.0037
103198_at	AI848576	Expressed sequence AI848576	AI848576	—	2.37	*1.52*	0.0040
104346_at	NM_028250	Acyl-coenzyme A binding domain containing 6	Abdc6	*1.06*	*1.70*	2.67	0.0040
98918_at	NM_145367	Thioredoxin domain containing 5	Txndc5	*−1.09*	*1.17*	2.69	0.0047
160754_at	NM_011224	Muscle glycogen phosphorylase	Pygm	—	*1.25*	4.28	0.0050
98957_at	NM_023277	Junction adhesion molecule 3	Jam3	*1.03*	2.03	3.31	0.0052
98967_at	NM_021272	Fatty acid binding protein 7, brain	Fabp7	*1.12*	3.27	7.28	0.0065
95356_at	NM_009696	Apolipoprotein E	Apoe	*−1.16*	2.23	*1.70*	0.0066
101855_at	NM_010837	Microtubule-associated protein 6	Mtap6	*−1.09*	*1.52*	2.98	0.0070

Continued

Table 1. *Continued*

Probeset	Accession no.	Gene description	Name	P2 AFC	P10 AFC	2M AFC	*P*-value
104643_at	XM_109956	KIBRA protein	Kibra	*1.13*	5.51	5.98	0.0070
93482_at	AK020638	RIKEN cDNA *9530072E15* gene	9530072E15Rik	*1.08*	2.17	2.78	0.0080
102682_at	NM_007939	Eph receptor A8	Epha8	*−1.04*	2.65	*1.22*	0.0080
160828_at	XM_148966	Inhibin beta-B	Inhbb	*1.26*	2.83	—	0.0080
103038_at	NM_008189	Guanylate cyclase activator 1a (retina)	Guca1a	*−1.21*	5.65	*1.45*	0.0115
99238_at	NM_013530	Guanine nucleotide binding protein, beta 3	Gnb3	*1.46*	2.75	5.34	0.0130
98852_at	NM_178280	Sal-like 3 (*Drosophila*)	Sall3	*1.23*	3.46	2.63	0.0130
93290_at	NM_013632	Purine-nucleoside phosphorylase	Pnp	*1.47*	2.97	4.22	0.0139
100453_at	NM_007595	Calcium/calmodulin-dependent protein kinase II, beta	Camk2b	*1.01*	2.30	3.11	0.0166
94338_g_at	NM_008087	Growth arrest specific 2	Gas2	*1.19*	10.07	*1.78*	0.0177
101344_at	NM_007627	Cholecystokinin B receptor	Cckbr	*1.04*	*1.44*	2.34	0.0177
95363_at	NM_008504	Granzyme M (lymphocyte met-ase 1)	Gzmm	—	3.16	4.82	0.0180
98560_at	NM_028870	Clathrin, light polypeptide (Lcb)	Cltb	*1.01*	2.43	3.71	0.0180
92904_at	NM_007548	PR domain containing 1, with ZNF domain	Prdm1	*1.13*	*1.40*	2.71	0.0300
102234_at	NM_024461	RIKEN cDNA *1810037I17* gene	1810037I17Rik	1.89	1.78	2.62	0.0314
92293_at	NM_176930	Neuronal cell adhesion molecule	Nrcam	*1.16*	*1.62*	2.27	0.0316
99111_at	NM_009191	Suppressor of K^+ transport defect 3	Skd3	*1.03*	2.25	2.23	0.0347
93973_at	NM_133916	Eukaryotic translation initiation factor 3, subunit 9 (eta)	Eif3s9	*−1.08*	*1.41*	2.24	0.0370
97206_at	NM_016907	Serine protease inhibitor, Kunitz type 1	Spint1	—	2.28	—	0.0380
98338_at	NM_010134	Engrailed 2	En2	*−1.02*	*1.04*	2.72	0.0426
92415_at	NM_009404	Tumor necrosis factor (ligand) superfamily, member 9	Tnfsf9	*1.05*	2.65	—	0.0479
101190_at	NM_008639	Melatonin receptor 1A	Mtnr1a	*1.18*	2.33	—	0.0566
96911_at	XM_282613	Guanine nucleotide binding protein, beta 2	Gnb2	*−1.01*	*1.30*	2.22	0.0566
160705_at	NM_007709	Cbp/p300-interacting transactivator w/E/D-rich carboxy-terminal dom 1	Cited1	*1.08*	2.34	*1.55*	0.0566
98424_at	NM_011204	Protein tyrosine phosphatase, non-receptor type 13	Ptpn13	*1.20*	*1.54*	2.24	0.0647
162206_f_at	NM_007707	Suppressor of cytokine signaling 3	Socs3	*1.14*	*1.62*	2.44	0.0650
96862_at	NM_134054	RIKEN cDNA *1110002B05* gene	1110002B05Rik	*1.24*	2.28	2.43	0.0670
94256_at	NM_013885	Chloride intracellular channel 4 (mitochondrial)	Clic4	*1.22*	*1.65*	2.28	0.0690
103033_at	NM_009780	Complement component 4 (within H-2S)	C4	*1.05*	*−1.11*	2.69	0.0700
101706_at	NM_009918	Cyclic nucleotide gated channel alpha 3	Cnga3	—	2.24	2.60	0.0780
93269_at	NM_025374	Glyoxalase 1	Glo1	*1.00*	*1.41*	2.15	0.0900
93731_at	NM_012056	FK506 binding protein 9	Fkbp9	*−1.19*	*1.48*	4.49	0.0910
96518_at	XM_109956	KIBRA protein	Kibra**	*1.09*	2.12	2.29	0.0934
103456_at	AW322500	Expressed sequence AW322500	AW322500	*−1.18*	2.69	2.34	0.1190
92232_at	NM_007707	Suppressor of cytokine signaling 3	Socs3**	*1.06*	*1.64*	2.37	0.1200
104374_at	NM_009252	Serine (or cysteine) proteinase inhibitor, clade A, member 3N	Serpina3n	—	—	2.82	0.1251
104564_at	NM_009130	Secretogranin III	Scg3	*1.13*	1.93	2.49	0.1251
103241_at	NM_153534	Adenylate cyclase 2	Adcy2	*1.34*	1.92	1.95	0.1350
94393_r_at	NM_019423	ELOVL family member 2, elongation of long chain fatty acids (yeast)	Elovl2	*1.33*	2.82	3.09	0.1370
92534_at	NM_010276	GTP binding protein (gene overexpressed in skeletal muscle)	Gem	*1.16*	*1.42*	2.82	0.1535
100026_at	NM_007532	Branched chain aminotransferase 1, cytosolic	Bcat1	*1.01*	*1.38*	1.96	0.1540
99972_at	NM_009414	Tryptophan hydroxylase 1	Tph1	—	*1.49*	2.15	0.1590
95105_at	NM_025933	RIKEN cDNA *2010110M21* gene	2010110M21Rik	*1.01*	*1.71*	2.06	0.1670
97722_at	NM_025965	Signal sequence receptor, alpha	Ssr1	2.17	2.03	1.96	0.1770
93268_at	NM_025374	Glyoxalase 1	Glo1**	*1.13*	*1.42*	2.34	0.2070
93669_f_at	NM_009234	SRY-box containing gene 11	Sox11	3.41	*1.75*	—	0.2220
94872_at	NM_020561	Acid sphingomyelinase-like phosphodiesterase 3a	Asml3a-pending	*1.04*	1.89	1.94	0.2220
99014_at	XM_133641	Amyloid beta (A4) precursor protein-binding, family B, member 1	Apbb1	*−1.01*	*1.58*	1.88	0.2550
93412_at	NM_010045	Duffy blood group	Dfy	*1.10*	*1.35*	1.94	0.2570
97124_at	NM_008016	Fibroblast growth factor inducible 15	Fin15	*1.16*	*1.90*	2.32	0.2940
104104_at	NM_030237	Spermatogenic Zip 1	Spz1-pending	*−1.20*	*1.20*	2.41	0.3120
94733_at	NM_008830	ATP-binding cassette, sub-family B (MDR/TAP), member 4	Abcb4	*1.05*	*1.37*	1.77	0.3140
104761_at	XM_132228	Anthrax toxin receptor	Antxr2	*1.13*	*1.18*	2.36	0.3275
101044_at	NM_008525	Aminolevulinate, delta-, dehydratase	Alad	*1.27*	1.90	1.82	0.3328

Continued

Table 1. *Continued*

Probeset	Accession no.	Gene description	Name	P2 AFC	P10 AFC	2M AFC	*P*-value
99623_s_at	NM_019498	Olfactomedin 1	Olfm1	*1.05*	*1.47*	2.18	0.3410
98544_at	NM_008193	Guanylate kinase 1	Guk1	*1.02*	*−1.01*	1.88	0.3819
98111_at	NM_013559	Heat shock protein 105	Hsp105	*1.18*	*1.06*	2.33	0.4600
92770_at	XM_192936	S100 calcium binding protein A6 (calcyclin)	S100a6	*1.13*	*1.09*	2.13	0.4870
101861_at	NM_011360	Sarcoglycan, epsilon	Sgce	*−1.03*	*1.38*	1.70	0.4890
104388_at	NM_011338	Chemokine (C–C motif) ligand 9	Ccl9	—	—	2.12	0.5800
160937_at	NM_016669	Crystallin, mu	Crym	*1.00*	*1.23*	1.99	0.6290
93354_at	NM_007469	Apolipoprotein C-I	Apoc1	—	1.82	—	0.6778
98005_at	NM_008862	Protein kinase inhibitor, alpha	Pkia	*1.07*	*1.25*	2.14	0.6870
101191_at	NM_007873	Double C2, beta	Doc2b	*−1.01*	*−1.04*	1.95	0.7286
104469_at	NM_010329	Glycoprotein 38	Gp38	*1.26*	*1.23*	2.10	0.7560
94258_at	NM_007486	Rho, GDP dissociation inhibitor (GDI) beta	Arhgdib	*1.09*	*1.08*	1.86	0.7801
160414_at	NM_024249	RIKEN cDNA *1810073N04* gene	1810073N04Rik	*1.01*	1.84	*1.36*	0.8697
95397_at	XM_196081	RIKEN cDNA *D430019H16* gene	D430019H16Rik	*1.04*	1.73	*1.63*	0.9320
93496_at	NM_134255	ELOVL family member 5, elongation of long chain fatty acids (yeast)	Elovl5	*−1.02*	*1.26*	1.96	0.9810

Differentially expressed genes are listed based on statistical ranking (FDRCI *P*-values) and all are shown with a *P*-value < 1 based on a 1.5 minfc MGU74Av2 probeset IDs and corresponding GenBank accession numbers (RefSeq if available) are given. Where multiple probesets correspond to a single gene, the additional probesets are indicated by asterisks and italicized text. AFC in expression in Nrl relative to wild-type is shown for the three time-points analyzed, P2, P10 and 2 months (2M) after signal quantification and normalization by RMA. Dashes indicate that gene expression was reported as absent (by MAS5) on all eight GeneChips for the given time-point (i.e. wild-type and $Nrl^{-/-}$). Italicized numbers indicate a non-significant AFC as determined by statistical analysis (*P*-value = 1). The lowest *P*-values are given for the three time-points measured for each of the gene probesets.

addition to a level of statistical significance. Although the highly differentially expressed genes are near the top of the lists as expected, the order is based on both the AFC and the variability of the signal data across the GeneChips. For this reason, probesets displaying a relatively high AFC for a given time-point may still be reported as non-significant [e.g. Nt5e (down-regulated) and Fin15 (up-regulated) at P10 in Table 1]. After removing probesets that belong to the same gene and show similar gene expression profile, a non-redundant set comprising 78 down-regulated and 83 up-regulated genes is obtained. Almost 90% of these genes are categorized as 'known', whereas 18 are novel sequences that are represented currently only in expressed sequence tag (EST) or genomic sequence databases.

Validation by quantitative real-time PCR

Fifty-four different gene/time-point values spanning a broad spectrum of AFC and FDRCI rankings were examined by quantitative real-time PCR (Q-PCR) (Table 2). There is a good correlation ($R^2 = 0.91$, data not shown) between AFC reported by microarray and by Q-PCR. Underestimation of the relative degree of fold-change in microarray data is likely due to background noise and limited sensitivity that restricts the dynamic range of this hybridization-based technique. Only three genes (*Gas5*, *Sox11* and *1110002B05Rik*) showed disagreement between the two methods (94% validation rate). The discrepancy could be due to the existence of multiple isoforms, which have been identified for these genes. The importance of validation is evident, not only for identifying possible false positives but also for determining the relative fold-change in transcripts (i.e. biological change) compared with the AFC reported by microarray. For example, Guca1a and Kibra are both predicted to be moderately up-regulated (5.6 and 6.0, respectively) in the $Nrl^{-/-}$ retina; however, Guca1a is shown to be up-regulated 5.5-fold by Q-PCR (same as microarray) but Kibra 26-fold (5-fold underestimate by microarray). Similar examples are evident amongst the down-regulated genes. Q-PCR analysis using additional retinal samples for six of the genes revealed similar AFCs (data not shown).

Hierarchical clustering and functional annotation

Relative expression profiling across multiple developmental time-points can provide information on the potential role of a given gene in the context of known biological events occurring within that time frame. Comparison of relative profiles can allow clustering of genes into groups that show similar patterns of behavior. To compare expression patterns between all 161 differentially expressed genes, the average signals from the four replicate GeneChips were first normalized to z-scores, and then run through a hierarchical clustering algorithm. Ten major clusters were identified by visual inspection, and Gene Ontology was used to assign functional annotation of 101 genes (62%) (Fig. 1).

Cluster I contains genes that display a bimodal (peaks at P2 and 2 month) or constant pattern of expression in wild-type, but show significantly decreased expression at P10 or 2 months of age in the $Nrl^{-/-}$ retina. Cluster II contains three γ-crystallin genes (E, D and F); for these, the peak expression is in the wild-type adult retina, but in the $Nrl^{-/-}$ retina there is increased expression at P2 and P10 but a significant decrease at 2 months. Although these genes show AFCs >2-fold at P10, none of these is considered statistically significant (Table 1). This may be due to the signal noise associated with the high degree of sequence identity between different crystallins. Q-PCR confirmed the decreased expression of Crygd and

Table 2. Real-time Q-PCR validation

Name	AFC	Q-PCR	*P*-value
Down-regulated genes			
Dpl1l	−15.9	−43.3	0.0001
Pdc6b	−25.0	−52.7	0.0002
Rho	−41.3	−1604.0	0.0003
Cnga1	−13.6	−406.4	0.0004
Gnb1	−8.1	−78.3	0.0004
Gas5	−6.3	−1.8	0.0008
Aqp1	−7.8	−52.3	0.0011
Mcf2c	−4.2	−4.6	0.0029
Gnat1	−216.4	−3494.4	0.0046
Cdr2	−5.5	−7.0	0.0080
Pdir-pending	−2.7	−14.3	0.0120
Pde6a	−3.0	−13.3	0.0160
Zfp36l2	−3.7	−7.7	0.0197
Rom1	−3.3	−5.7	0.0280
2900026H06Rik*	−3.2	−4.7	0.0340
Wisp1	−3.3	−32.7	0.0479
Tnfaip3	−4.5	−7.5	0.0580
D6Wsu176e	−3.3	−9.2	0.0650
D1Ertd622e	−2.5	−7.7	0.0934
Abca4	−2.2	−6.6	0.1081
Mpdz	−2.6	−7.9	0.1084
0610012A05Rik	−2.7	−3.6	0.2140
Mbnl1*	−2.0	−2.2	0.2530
Lmo1	−1.9	−9.6	0.2940
Drd4*	−4.5	−12.7	0.3410
Crygf	−3.5	−4.8	0.4940
Crygd	−3.2	−6.5	0.7652
Up-regulated genes			
Clca3	14.9	44.2	0.0003
Opn1sw	9.4	23.1	0.0004
Casp7	6.4	10.7	0.0017
Gnat2	7.6	15.3	0.0029
Txndc5	2.7	7.8	0.0047
Fabp7	7.3	49.1	0.0065
Epha8*	2.6	10.1	0.0080
Inhbb*	2.8	9.5	0.0080
Rxrg	2.9	8.9	0.0108
Guca1a*	5.6	5.5	0.0115
Kibra	6.0	26.0	0.0120
Gnb3	5.3	8.2	0.0130
Sall3	2.6	2.4	0.0130
Camk2b	3.1	15.6	0.0166
Gas2*	10.1	52.8	0.0177
Sall3*	3.5	20.8	0.0180
Gzmm	4.8	2.5	0.0180
Prdm1	2.7	7.6	0.0300
1810037I17Rik	2.6	2.1	0.0314
En2	2.7	31.3	0.0426
Socs3	2.4	19.7	0.0650
Serpina3n	2.8	3.2	0.1251
Elovl2	3.1	5.1	0.1370
1110002B05Rik	2.4	1.2	0.1880
Sox11**	3.4	−2.0	0.2220
Antxr2	2.4	7.0	0.3275
Olfm1	2.2	2.0	0.3410

AFC is based on the microarray data with corresponding FDRCI *P*-value. Relative fold-change based on Q-PCR is shown. All measurements were on adult (2M) retina except where indicated (**P2, *P10). Underlined values indicate genes for which there are significant discrepancies between the two methods [i.e. no significant change reported by Q-PCR (<2-fold) or direction of change is in disagreement with microarray data].

Crygf at 2 months (Table 2). Crystallins are expressed in neural retina and may play a role in stress response (33). For the genes of Cluster V, their expression peaks at P10 but then decreases (though still detectable) in the wild-type adult retina. In the $Nrl^{-/-}$ retina, the peak expression may still be at P10, but is reduced for all these genes, suggesting a potential role in differentiation, as indicated for Ndr1, Ndrl and Lmo1. Cluster VI contains only two ESTs that are expressed across all three time-points but are down-regulated in the $Nrl^{-/-}$ retina.

Almost 80% of genes showing decreased expression in the $Nrl^{-/-}$ retina belong to clusters III and IV. These genes demonstrate an increasing (relative) level of expression, reaching peak expression by P10 (cluster III) or 2 months (cluster IV) in wild-type, suggesting a role in the mature retina/photoreceptors. In the $Nrl^{-/-}$ retina, these genes are down-regulated showing, typically, only a moderate (or no) increase in expression at later time-points. Genes of these clusters are strong candidates for direct positive regulation by Nrl and include Rho, Pdc6b and Pde6a (known targets of Nrl) as well as Gnat1 and Gnb1.

The genes showing higher expression in the $Nrl^{-/-}$ retina can be organized into four major clusters. The genes of the largest cluster VIII show an increase in expression at P10 or 2 months in the $Nrl^{-/-}$ retina relative to wild-type. As anticipated, this includes genes encoding proteins with a role in cone-mediated visual function (e.g. Opn1sw and Gnat2). Expression of cluster VII genes peaks at P2 in wild-type, suggesting a primary role in early development, but in the $Nrl^{-/-}$ retina they show elevated expression peaking at P10 or 2 months. Their sustained high expression in the adult retina may be indicative of an aberrant reactivation of gene expression, possibly related to stress, cell death or reactive gliosis. Cluster IX genes show an elevated differential expression (and peak) in the $Nrl^{-/-}$ retina, primarily at P10, and may play a role in cone differentiation. Of the 14 genes in this cluster, six are associated with signaling, development or cell cycle/growth. Cluster X includes genes showing peak expression at P2 in wild-type but the expression declines (often rapidly) by P10 or 2 months, suggesting a primary role in early development. In the $Nrl^{-/-}$ retina, the expression profile is similar but the expression is elevated and maintained for a longer period.

Direct targets of Nrl identified by ChIP

We hypothesized that targets of Nrl will be enriched among the genes exhibiting reduced expression in the $Nrl^{-/-}$ retina. Hence, we examined the enrichment of the promoter regions that include a potential AP-1 like or Nrl-response element (NRE) of 'candidate Nrl targets' by ChIP with a polyclonal anti-Nrl antibody (8) using the wild-type mouse retina. Twenty different gene promoters were assayed by PCR amplification; of these, 18 (90%) showed enrichment in the antibody fractions (Nrl-ChIP) over the no antibody control (Fig. 2), demonstrating *in vivo* promoter occupancy by Nrl. The positive target promoters included three genes (*Rho*, *Pde6b* and *Pde6a*) that are modulated by Nrl. The promoters of other photoreceptor genes (such as *Cnga1*, *Gnat1*, *Gnb1*, *Rom1* and *Pdc*) were also enriched. In addition, a few widely expressed genes, such as *Aqp1* (water channel) and adiponectin receptor 1 (*AdipoR1*), appear to be the target of Nrl

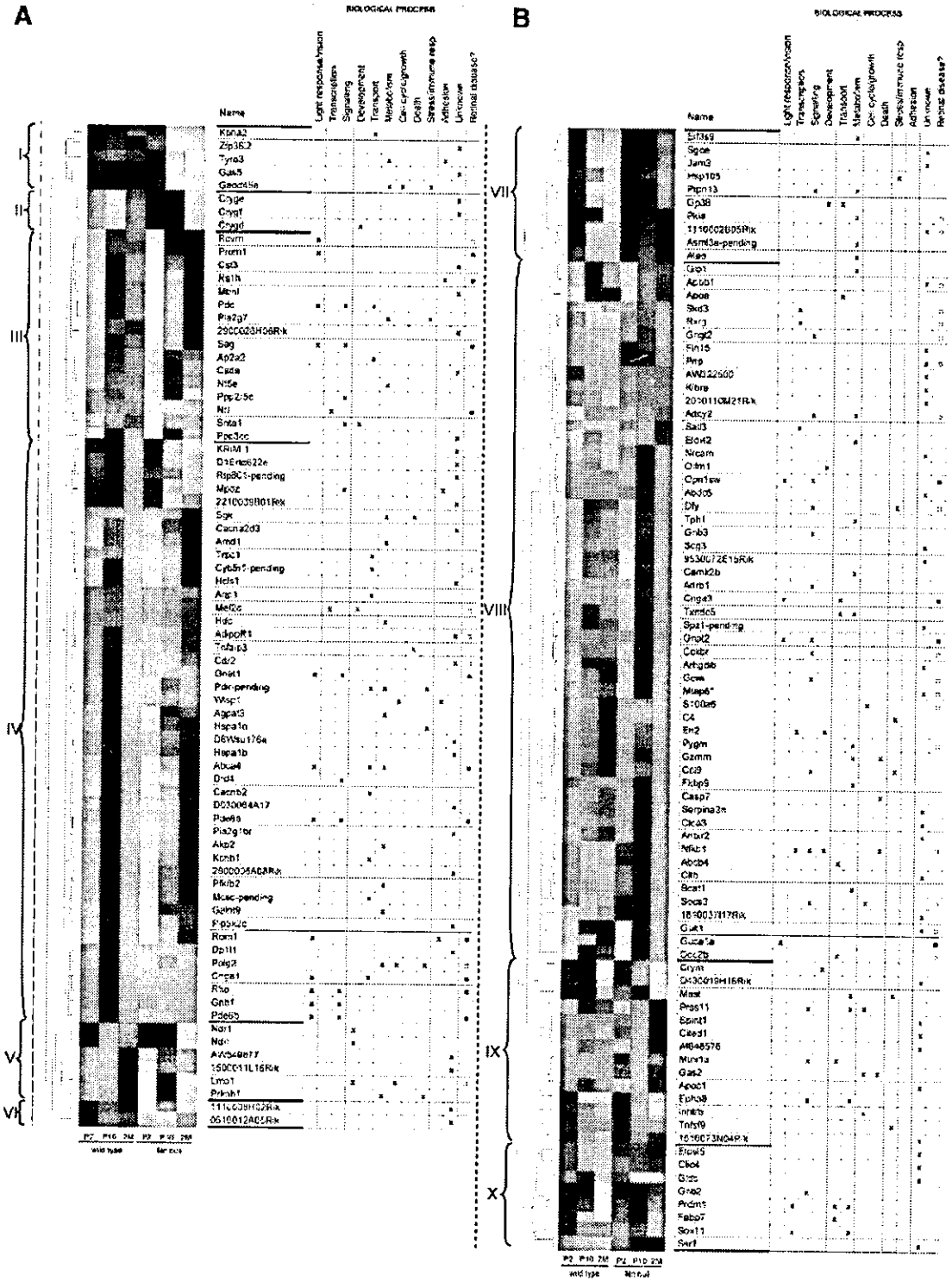

Figure 1. Hierarchical clustering and functional annotation. Clustering of differentially expressed genes based on normalized average signals (z-scores). Bright green boxes indicate lowest signal with increasing values indicated by darkening color towards bright red, representing peak signal. The set of 161 non-redundant genes are divided, based on similarity of profiles, into 10 clusters. **(A)** Down-regulated genes are in groups I–VI and **(B)** up-regulated in groups VII–X. Functional annotation is based on defined biological processes assigned by the Gene Ontology (GO) consortium. Though listed as having no defined function, Mtap6 (indicated by an asterisk) is associated with microtubules and has a presumed role in synaptic plasticity and function. The far right column indicates whether the gene is known to be associated with (black square) or is a candidate for (empty square) retinal disease (see Table 3 also).

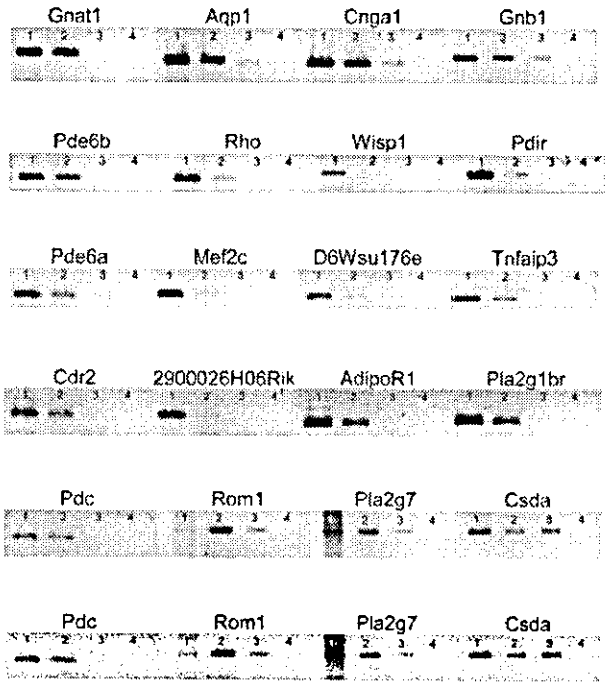

Figure 2. ChIP analysis. PCR products are shown for 20 different gene promoters in which the most proximal putative AP-1/NRE-like site was assayed. Each set includes the input genomic DNA as positive control (lane 1), chromatin DNA fraction immunoprecipitated with anti-NRL antibody (lane 2), chromatin DNA obtained without the antibody (background control; lane 3) and water (negative control; lane 4). Enrichment (greater amount of product) with antibody IP over background control (no Ab) indicates the *in vivo* occupancy of a sequence element within the amplified region by Nrl. All assayed gene promoters showed enrichment, except Wisp1 (inconclusive) and Csda (negative). Direct regulation of Rho and Pde6b by Nrl (at these sites) has been demonstrated previously, and as such these are positive controls for the ChIP protocol.

regulation in mature rods. It should be noted that although only down-regulated genes were analyzed by ChIP, Nrl might negatively regulate (i.e. repress) the expression of cone-specific genes, much akin to the predicted role of Nr2e3 (21).

Identification of retinal disease candidate genes

Many genes showing photoreceptor-enriched expression are associated with retinal disease; these encode diverse functions, including phototransduction (e.g. rhodopsin), transcriptional regulation (e.g. *Crx* and *Nrl*), outer segment structure (e.g. *Rom1* and *Prom1*) or maintenance of the extracellular matrix (e.g. *Rs1h*). Expression profiling of a mouse model with retinal degeneration ($Rho^{-/-}$) was utilized previously to identify a retinitis pigmentosa disease gene (*RP10*), inosine monophosphate dehydrogenase type 1 (IMPDH1) (34), which was not an obvious candidate due to its ubiquitous expression and role in guanosine nucleotide biosynthesis. We, therefore, determined the chromosomal location of genes that are expressed differentially in the $Nrl^{-/-}$ retina using *in silico* methods. On the basis of the map position of the human homolog, 41 of the differentially expressed genes (25%) have been associated previously with or are candidates for retinal diseases (Table 3). A few of these (e.g. *Mef2c*, *Nt5e* and *Cdr2*) were also identified in the $Rho^{-/-}$ gene profiling study (34), providing further evidence of their rod-preferred expression. Up-regulated genes that are candidates for macular or cone associated diseases include *S100A6*, *RXRG*, *ADCY2*, *NP* and *SOCS3*, whereas down-regulated genes that map to the region of rod associated disease loci (such as RP) include *NT5E* and *CDR2*.

Analysis of differentially expressed genes

Light response and vision. The genes displaying restricted expression to rods or cones show the most dramatic changes in expression. For the rods, these include genes encoding rod-specific phototransduction proteins such as rhodopsin (Rho), cGMP phosphodiesterase subunits (Pde6a and b), rod transducin subunits (Gnat1 and Gnb1) and the cyclic nucleotide gated channel subunit (Cnga1). By Q-PCR, transcripts of these genes are virtually undetectable in the $Nrl^{-/-}$ retina with expression typically $<1\%$ of wild-type. Modest expression of Pde6a ($\sim 7\%$) and Pde6b ($\sim 2\%$) in the adult $Nrl^{-/-}$ retina can be attributed to their expression in non-photoreceptor neurons, as observed for Pde6a (35). Genes encoding cone phototransduction proteins, such as the photopigment S-opsin (Opn1sw), cone transducin subunits (Gnat2, Gnb3 and Gngt2) and the cyclic nucleotide gated channel subunit (Cnga3), show dramatically higher expression in the $Nrl^{-/-}$ retina. A number of genes that are expressed in both photoreceptor subtypes show varying degrees of expression change, which may reflect a moderate quantitative bias towards one class (or expression in multiple cell types). These include guanylate cyclase activator 1a (Guca1a or Gcap1), recoverin (Rcvrn), prominin 1 (Prom1), phosducin (Pdc), retinal S-antigen (Sag), retinal outer segment membrane protein (Rom1) and an ATP-binding cassette (ABC) transporter (Abca4). Guca1a displays a 5.5-fold increase in expression in the $Nrl^{-/-}$ retina suggesting preferential expression in cones. Notably, although expressed in both rods and cones, mutations in this gene are primarily associated with cone or cone–rod dystrophies (36,37). Other down-regulated genes may indicate their preferential expression in rods.

Gene regulation, differentiation and development. Transcription factors and signaling molecules that are expressed differentially in the $Nrl^{-/-}$ retina may provide insights into the regulatory networks associated with photoreceptor development and/or function. Q-PCR analysis of E14–P21 retina for the cone photopigment Opn1sw (S-opsin) showed that the increase in its expression occurred at P6.5 in the $Nrl^{-/-}$ retina (Fig. 3). This second-wave of cone differentiation likely corresponds to the post-mitotic photoreceptors that are normally destined to become rods. Therefore, it is predicted that genes associated with rod or cone differentiation would be down- or up-regulated, respectively, at this time-point. The expression of MADS-box containing myocyte enhancer factor 2c (Mef2c) (38,39) is reduced in the matured $Nrl^{-/-}$ retina to 20% of the wild-type levels. Zfp36l2 (a C3H-type zinc finger protein) is down-regulated $\sim$8-fold in the $Nrl^{-/-}$ retina. A significant decrease in expression of LIM domain only 1 (Lmo1), a developmentally associated transcription factor, is observed in the adult retina (10-fold by Q-PCR) suggesting its role in mature rods. Similar profiles are also